THE JOURNAL OF PHYSICAL CHEMISTRY B

Article

pubs.acs.org/JPCB

A Bioelectrochemical Method for the Quantitative Description of the Hofmeister Effect of Ionic Liquids in Aqueous Solution

Lu Lu,[†] Yan Hu,[†] Xirong Huang,*[,†,‡] and Yinbo Qu[‡]

[†]Key Laboratory of Colloid & Interface Chemistry of the Education Ministry of China, Shandong University, Jinan 250100, People's Republic of China

[‡]State Key Laboratory of Microbial Technology of China, Shandong University, Jinan 250100, People's Republic of China

Supporting Information

ABSTRACT: It is imperative to establish a simple, efficient, and practical method to investigate the Hofmeister effect of ionic liquids (ILs) on the behavior of proteins (enzymes). In this study, the effects of the cations and anions of different ILs in aqueous media on the structural stability of horseradish peroxidase (HRP), a model oxidoreductase, were systematically investigated using electrochemical methods. It is found that without ILs no direct electron transfer current signals of HRP appear at bare glassy carbon electrode (GCE) in phosphate buffer (pH 7.0) even after incubation and accumulation at a negative potential. In the presence of ILs, however, a current signal occurs at GCE, depending on the structure of the IL and its concentration. A linear relationship between the peak currents and the scan rates demonstrates that the direct electron transfer is a surface-confined thin-layer electrochemical process. The redox signal at GCE is from the heme of HRP. An IL has a perturbing effect on the HRP structure. The anodic peak current of HRP at GCE, the catalytic activity of HRP, and the secondary structure of HRP are well correlated. Different cations or anions at varied concentrations have different effects on the structural stability of HRP, resulting in different current signals at GCE. Thus, the anodic peak current of HRP at GCE can be used as an indicator to quantitatively characterize the effect of ILs on the structural stability of HRP. The present Hofmeister series for cations and anions is in good agreement with that reported elsewhere. To our knowledge, this is a first attempt to establish a simple and practical electrochemical method to correlate Hofmeister effects with characteristics of ions and solvents. The present investigation not only deepens our understanding of the complex electrochemical behavior of proteins in ILs media but also offers a practical guidance to designing "green" and biocompatible ILs for protein (enzyme) separation, purification, and enzymatic catalysis and conversion.

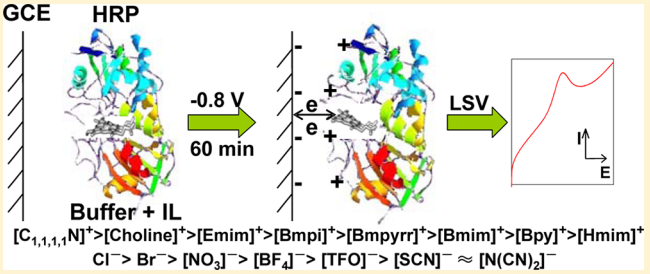

INTRODUCTION

Proteins are composed of amino acids. Their structure and function is thus destined to be influenced by the electrolytes in aqueous solutions. The Hofmeister series[1] for common inorganic ions reflects the effects of cations and anions in aqueous media on the structural stability of proteins.[2] The Hofmeister series has played an important role in guiding protein (enzyme) separation, purification, and enzymatic catalysis and conversion;[3] though the mechanism of the Hofmeister effect is not quite clear at present.

Ionic liquids (ILs) are molten salts that consist of organic cations and organic/inorganic anions. In recent years, the interaction between ILs and proteins (enzymes) has attracted considerable attention due to the unique physicochemical properties of ILs such as "green" property and designability. It has been shown that ILs affect the stability of proteins,[4−7] the catalytic activity of enzymes,[8−10] the enantioselectivity of enzymes,[11] and so on. A study on the Hofmeister effect of the cations and anions of ILs has been a hot issue recently. In comparison with inorganic ions, the diversity and complexity of organic ions' structure makes the investigation of their Hofmeister effect difficult. Differential scanning fluorimetry,[12] steady-state fluorescence spectroscopy,[13] circular dichroism (CD) spectroscopy,[5] and differential scanning calorimetry[14] have been used to quantitatively correlate the Hofmeister effect of ILs with the characteristics of ions and solvents. In their methodologies, the optical and thermal properties of the protein (enzyme)/IL systems are utilized; however, the electrochemical properties of the systems have not been tried to make such quantitative correlation.

As is well known, ILs have been widely used in electrochemical science due to their good conductivity and wide electrochemical window.[15] People have observed the effects of ILs on the direct electron transfer process between the immobilized redox proteins (enzymes) and the electrodes. It has been found that the effects are closely correlated with not only the nature and usage of ILs but also the type of proteins used. Most of the results indicate that ILs can facilitate the

Received: June 2, 2012
Revised: August 11, 2012
Published: August 16, 2012

dx.doi.org/10.1021/jp3054263 | J. Phys. Chem. B 2012, 116, 11075−11080

direct electrochemistry of redox proteins,[16] but there are some reports showing that ILs have little effects[17] or negative effects.[18] However, few people pay attention to the direct electrochemistry of free redox proteins (enzymes) in ILs aqueous solutions and a systemic study has not been reported so far.

As one of the heme-containing proteins, horseradish peroxidase (HRP) is a monomeric glycoprotein with a molecular weight of ca. 44 kDa.[19] In this paper, HRP is chosen as a model protein. When dissolved in a phosphate buffer containing different kinds and varied concentrations of hydrophilic ILs, we observed that ILs facilitated the direct electron transfer between HRP and a glassy carbon electrode (GCE) and the observed currents were correlated with the kinds and the concentrations of ILs. CD spectroscopy and enzyme kinetics demonstrated that it was caused by the effects of the ILs on the structural stability of HRP.[11,20] On the basis of such effects, the Hofmeister series of hydrophilic ILs were established using this novel electrochemical method, which is simple, sensitive, and efficient. From the perspective of the basic research, the present work deepens our understanding of the behaviors of the proteins in ILs media, and it also provides scientific guidance for the selection of ILs that could stabilize a specific protein.

EXPERIMENTAL SECTION

Material. HRP (EC 1.11.1.7, 250 U mg^{-1}), guanidine hydrochloride and *o*-phenylenediamine (OPD) were purchased from Sinopharm Chemical Reagent Co. Ltd. The ILs containing the same anion are 1-ethyl-3-methylimidazolium tetrafluoroborate ([Emim][BF_4]), 1-butyl-3-methylimidazolium tetrafluoroborate ([Bmim][BF_4]), 1-hexyl-3-methylimidazolium tetrafluoroborate ([Hmim][BF_4]), 1-butyl-1-methylpiperidinium tetrafluoroborate ([Bmpi][BF_4]), 1-butylpyridinium tetrafluoroborate ([Bpy][BF_4]), 1-butyl-1-methylpyrrolidinium tetrafluoroborate ([Bmpyrr][BF_4]), tetramethylammonium tetrafluoroborate ([$C_{1,1,1,1}N$][BF_4]) and choline tetrafluoroborate ([Choline][BF_4]). The ILs containing the same cation are 1-butyl-3-methylimidazolium chloride ([Bmim]Cl), 1-butyl-3-methylimidazolium bromide ([Bmim]Br), 1-butyl-3-methylimidazolium tetrafluoroborate ([Bmim][BF_4]), 1-butyl-3-methylimidazolium dicyanimide ([Bmim][$N(CN)_2$]), 1-butyl-3-methylimidazolium thiocyanate ([Bmim][SCN]), 1-butyl-3-methylimidazolium nitrate ([Bmim][NO_3]), and 1-butyl-3-methylimidazolium trifluoromethanesulfonate ([Bmim][TFO]). The aforementioned ILs (99%) were provided by Shanghai Chengjie Chemicals Co. Ltd. and used without further purification. 0.01 and 0.1 M phosphate buffer (pH 7.0) were prepared by mixing stock standard solutions of Na_2HPO_4 and NaH_2PO_4 and adjusting the pH with 0.01 or 0.1 M H_3PO_4 or NaOH. HRP stock solution (10 mg mL^{-1}) was prepared by dissolving HRP in the phosphate buffer. For concentrated [Bmim][TFO], the IL-containing phosphate buffers were readjusted to pH 7.0 prior to use. All other reagents were of analytical grade and used as received. Triply distilled water was used throughout the experiments.

Pretreatment of GCE. A GCE (3 mm in diameter) was first polished with 500 and 50 nm alumina slurry on chamois leather. After that, it was cleaned sequentially in an ultrasonic cleaner with 1:1 (V/V) nitric acid, acetone, and triply distilled water for 5 min, respectively. Finally, the GCE was dried with nitrogen gas.

Electrochemical Measurements. Cyclic voltammetry and linear sweep voltammetry were performed on a CHI 630C Electrochemical Analyzer (Shanghai Chenhua Co., China). The three-electrode system was composed of a working electrode (GCE), a platinum wire counter electrode, and a saturated calomel electrode (SCE) reference electrode. Prior to measurements, the phosphate buffers (pH 7.0) containing different kinds and varied concentrations of ILs were deaerated with high purity nitrogen sufficiently. The HRP stock solution was then added into the oxygen-free electrolytes (the optimum final concentration was 50 μM). HRP was incubated and accumulated at a negative potential in the electrolytes under constant bubbling of nitrogen for a fixed time (60 min). Before electrochemical measurements, the system was set at rest for 30 s. During the experiment, the system was kept under nitrogenous atmosphere. For cyclic voltammetric experiments, only the first cycle was recorded. All the potentials given in this paper were vs SCE. The electrochemical measurements were carried out at 17 ± 1 °C.

Spectroscopic Records. CD spectra of HRP (50 μM) in far-ultraviolet (UV) region (200−260 nm) were recorded on a J-810 CD spectrometer (Jasco, Japan) using a 1.0-mm quartz cuvette. Prior to measurements, the HRP solutions containing different concentrations of different ILs were incubated for 60 min. Each spectrum was baseline-corrected, and the final spectrum was an average of triplicates. The spectroscopic measurements were carried out at 17 ± 1 °C.

Determination of HRP Activity. The activity of HRP in the phosphate buffer (pH 7.0) with different concentrations of ILs ([$C_{1,1,1,1}N$][BF_4] or [Choline][BF_4]) was determined using a UV−visible spectrophotometer (UV-2550, Shimadzu). Prior to determinations, the HRP solutions (50 μM) containing different concentrations of ILs were incubated for 60 min. A 10-μL aliquot of the instantly diluted HRP solution (50 μM) was used to initiate the HRP-catalyzed oxidation of OPD at pH 7.0 in a 3 mL quartz cuvette at 30 ± 1 °C. The final concentrations of OPD and H_2O_2 were 3.0 and 1.5 mM, respectively. The reaction was monitored by tracing the time dependent change in absorbance at 448 nm. The molar extinction coefficient of the oxidation product of OPD at 448 nm was 10.6 mM^{-1} cm^{-1}.[21] Each activity datum was an average of triplicate measurements with relative deviation less than 5%.

RESULTS AND DISCUSSION

Electrochemical Behaviors of HRP in IL Aqueous Solutions. Figure 1 shows the cyclic voltammograms of HRP (50 μM) in the phosphate buffer in the absence (dashed line) and presence (solid line) of 0.5 M [Bmim][BF_4]. It is seen that no redox peaks of HRP at GCE appear in the buffer without ILs; however, a pair of well-resolved redox peaks are observed in the IL-containing buffer. The results indicate that the direct electron transfer happens between HRP and GCE; moreover, it is a quasireversible process based on the peak potential separation (60 mV) and the peak current ratio (1.1). The redox process observed in the IL-containing buffer is attributed to the heme transformation between ferrous iron and ferric iron. For further demonstration, we investigated the electrochemical behavior of the denatured HRP at GCE in the buffer without ILs. The HRP aqueous solution (pH 7.0) was first heated at 90 °C for 10 min, followed by cooling down to the room temperature. The cyclic voltammogram of the denatured HRP at GCE in the buffer without ILs was then recorded (the dash dotted line). As seen from Figure 1, the denatured HRP has

dx.doi.org/10.1021/jp3054263 | J. Phys. Chem. B 2012, 116, 11075−11080

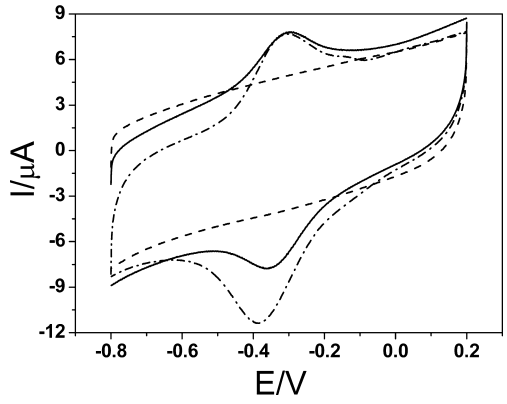

Figure 1. Cyclic voltammograms of HRP (50 μM) at GCE in 0.1 M phosphate buffer (pH 7.0) in the absence (dashed line for native HRP and dash dotted line for denatured HRP) and presence (solid line) of 0.5 M [Bmim][BF_4]. Scan rate: 1.0 V s^{-1}. The incubation time was 60 min.

two obvious peaks at GCE and the peak current is much bigger than that in the buffer containing 0.5 M [Bmim][BF_4]. A similar result was observed when HRP was denatured by guanidine hydrochloride (see Figures S1 and S2 of the Supporting Information). The comparison shows that the redox signal is really from the heme of HRP and that the larger exposure extent of the heme due to the denaturation treatment[22] results in a bigger signal. Usually, the direct electron transfer of HRP at bare conventional electrodes is not observed due to the deep burial of its electroactive center.[23] The present results show that the IL plays an important role in achieving the direct electrochemistry of HRP at bare GCE. The real mechanism of the effect is not clear now,[24] but our experimental results show that it is correlated with the structural stability of HRP in the presence of the ILs (especially the hydrophilic ILs). It is the interaction between the IL and HRP that changes the conformation of HRP and thus, to some extent, the microenvironment of the electroactive center, which exposes the heme to the solution. With the help of electrostatic and hydrophobic interactions between the HRP and the electrode, the HRP molecules are confined to the surface of GCE, which makes the direct electrochemistry of HRP at GCE go easily.

Spectroscopic Characterization of HRP in IL Aqueous Solutions. To explain the interaction between IL and HRP, CD spectroscopy was used to investigate the effects of IL at different levels on the secondary structure of HRP.[25] As the imidazolium-based ILs have a large CD background in the far-UV region,[26] especially at their high concentrations, the effects of [$C_{1,1,1,1}$N][BF_4] and [Choline][BF_4] at different concentrations on the secondary structure of HRP were investigated.[27] Parts A and B of Figure 2 show the CD spectra of HRP with or without ILs in the far-UV region. It is seen in Figure 2A that over the concentration range studied [$C_{1,1,1,1}$N][BF_4] has little influence on the secondary structure of HRP, and accordingly no direct electron transfer current of HRP can be observed in the subsequent electrochemical experiments. For [Choline]-[BF_4], however, with the increase of the concentration of [Choline][BF_4], the negative peak of HRP is red-shifted and the peak intensity weakens gradually. The subsequent electrochemical experiment shows an obvious direct electron transfer current of HRP, indicating that the effect of ILs on the secondary structure of HRP depends upon the type of an IL as

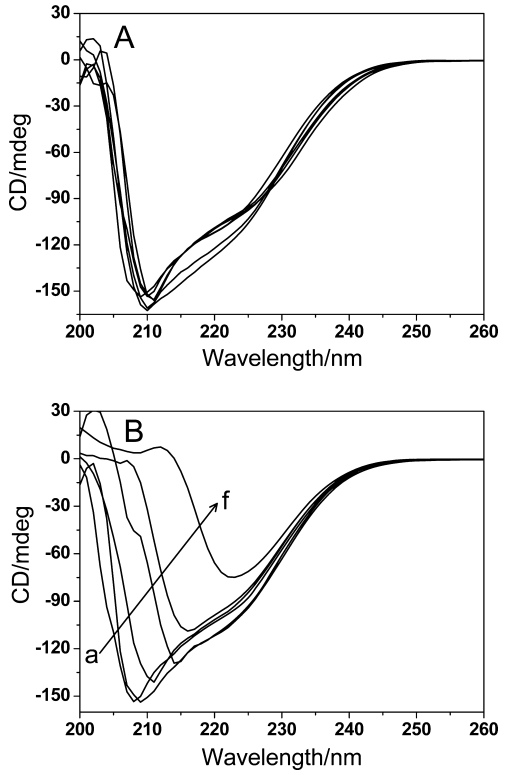

Figure 2. CD spectra of HRP (50 μM) in 0.01 M phosphate buffer (pH 7.0) with different concentrations of [$C_{1,1,1,1}$N][BF_4] (A) and [Choline][BF_4] (B) (a–f: 0, 0.2, 0.4, 0.6, 0.8, and 1.0 M).

well as its concentration and that the conformation of HRP is correlated with its current signal at GCE.

Effects of ILs on the Activity of HRP. To further correlate the peak current of HRP at GCE with the effect of ILs on the structural stability of HRP, the effects of the two ILs ([$C_{1,1,1,1}$N][BF_4] and [Choline][BF_4]) on the catalytic activity of HRP were also investigated. Figure 3 shows the relative activity and the anodic peak current of HRP as a function of the IL concentration. It is seen that over the concentration studied [$C_{1,1,1,1}$N][BF_4] has almost no effect on the activity of HRP and the anodic peak current, indicating that the structure of HRP is

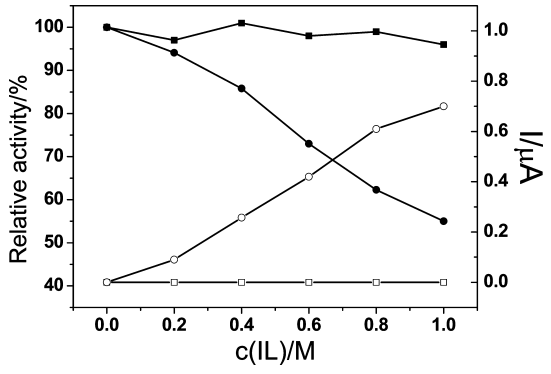

Figure 3. The relative activity of HRP (solid symbols) and the anodic peak current of HRP at GCE (hollow symbols) as a function of the concentration of [$C_{1,1,1,1}$N][BF_4] (square) and [Choline][BF_4] (circle). The relative activity (%) refers to the percentage of the initial rate of HRP-catalyzed oxidation of OPD at 448 nm in the presence of IL with respect to the one in the absence of IL (16 μM min^{-1}).

dx.doi.org/10.1021/jp3054263 | J. Phys. Chem. B 2012, 116, 11075–11080

not perturbed by this IL (the CD spectra of HRP in Figure 2A also supports this), and therefore no electron transfer between HRP and GCE happens. For [Choline][BF_4], however, it decreases the activity of HRP; the more the IL, the lower the activity, and the larger the anodic current. This means that [Choline][BF_4] has perturbed the conformation of HRP (this is supported by the CD spectra of HRP in Figure 2B), which makes the electron transfer easy to take place. All above results indicated that the anodic peak current of HRP at GCE, the catalytic activity of HRP and the secondary structure of HRP are all correlated; i.e., the anodic peak current of HRP at GCE can be used as an indicator to quantitatively characterize the effect of ILs on the structural stability of HRP.

Exploration of the Direct Electron Transfer Process of HRP at GCE. Figure 4 shows the linear sweep voltammograms

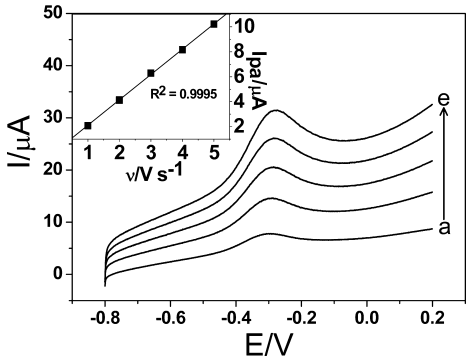

Figure 4. Linear sweep voltammograms of HRP (50 μM) at GCE in 0.1 M phosphate buffer (pH 7.0) containing 0.5 M [Bmim][BF_4] over a range of scan rates (a–e: 1.0, 2.0, 3.0, 4.0, and 5.0 V s^{-1}). Inset: plot of anodic peak currents vs scan rates. The incubation time was 60 min.

of HRP at GCE at different scan rates in phosphate buffer containing 0.5 M [Bmim][BF_4]. The redox peak currents increase proportionally to the increase of the scan rate, indicating that it is a surface-confined thin-layer electrochemical process.[28] For a reversible surface reaction, the peak current (I_p) is given by the equation[29]

$$I_p = \frac{n^2F^2A\Gamma\nu}{4RT}$$

where n is the number of electrons transferred, A is the surface area (0.071 cm^2) of the electrode, ν is the scan rate (V s^{-1}), and the other symbols have their usual meanings. The surface coverage (Γ) of HRP can be calculated from the slope of the curve of the anodic peak current (I_{pa}) vs the scan rate (see the inset in Figure 4). In this system, the Γ value is calculated to be $(2.95 \pm 0.10) \times 10^{-11}$ mol cm^{-2} (triplicate determinations). It can be concluded that the affected HRP molecules are confined to the surface of GCE via electrostatic and hydrophobic interactions between the HRP and the electrode, thereby facilitating the direct electrochemistry of HRP. The surface coverage of HRP in the presence of other ILs can be obtained similarly. It is worth a mention that the size of the affected HRP molecules is very different from that of the native ones due to the change of the conformation and for those affected HRP molecules that are far from the surface of electrode their direct electron transfer process does not happen. Therefore, the surface coverage obtained here is an apparent indicator that reflects the influencing ability of the ILs on the structure of HRP.

The Hofmeister Series for ILs. Figure 5A shows the linear sweep voltammograms of HRP at GCE in phosphate buffer

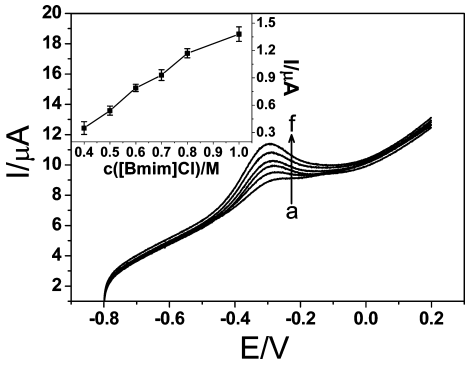

Figure 5. Linear sweep voltammograms of HRP (50 μM) at GCE in 0.1 M phosphate buffer (pH 7.0) containing different concentrations of [Bmim]Cl (a–f: 0.4, 0.5, 0.6, 0.7, 0.8, and 1.0 M) at a scan rate of 1.0 V s^{-1}. Inset: Effect of the concentrations of [Bmim]Cl on the anodic peak curents of HRP at the GCE.

containing different concentrations of [Bmim]Cl. It is seen that for a given concentration of HRP the anodic peak current increases with the increase of the IL concentration in the electrolyte, i.e., the effect of the IL on the structural stability of HRP is reflected by the direct electron transfer current signal at GCE (see the inset). The larger the anodic peak current, the larger the influencing ability of the ions. The Hofmeister series is therefore obtained by ranking the cations or anions of ILs according to the anodic peak current.

The $[BF_4]^-$-based ILs with different cations and the $[Bmim]^+$-based ILs with different anions were ranked. The electrolyte containing relatively low IL concentrations ($\leq$1.0 M) was investigated here to avoid obvious change of the physical properties of the system caused by the presence of high IL concentrations. For a given IL, several IL concentrations were investigated to distinguish between it and other ILs that give rise to a very close current.

Figure 6 shows the effect of the different $[BF_4]^-$-based ILs on the anodic peak current at GCE. In neat buffer or without any IL, the anodic peak current was 0. In the presence of an IL, an anodic peak current was observed, depending on the type of the IL and its concentration in the buffer. At a level of 0.2 M IL, [$C_{1,1,1,1}$N][BF_4] resulted in the least signal, but [Hmim][BF_4] gave rise to the largest signal. For clarity, the curve of [Hmim][BF_4] was given in Figure 6B separately. For the ILs studied, a similar varying trend of I vs [IL] was observed. The fact that the current increment decreases at a higher level of an IL does not mean that the signal reaches its maximum, because the current of the denatured HRP in the IL-free buffer is larger than that of the one in the buffer containing high level of an IL. Both the exposure extent of the heme in HRP and the number of HRP molecules that involve in direct electron transfer at GCE contribute to the current signal. The effects of these factors are relatively complicated, but they do not hinder the ranking.

In terms of the structural stability of HRP, the Hofmeister effect of the different cations is ranked in the following order:

dx.doi.org/10.1021/jp3054263 | J. Phys. Chem. B 2012, 116, 11075–11080

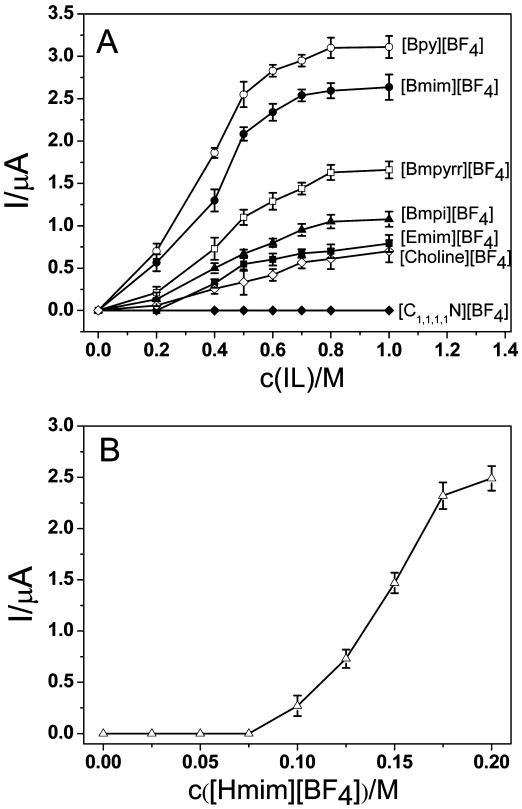

Figure 6. Effects of the concentrations of different cations on the anodic peak currents of HRP at the GCE. The concentration of HRP in the electrolyte was 50 μM, and the incubation time at each IL concentration was 60 min. Scan rate: 1.0 V s^{-1}.

$$[C_{1,1,1,1}N]^+ > [\text{Choline}]^+ > [\text{Emim}]^+ > [\text{Bmpi}]^+ > [\text{Bmpyrr}]^+ > [\text{Bmim}]^+ > [\text{Bpy}]^+ > [\text{Hmim}]^+$$

This Hofmeister series is consistent with that ranked based on the effects of ILs on the thermal stability of ribonuclease A using differential scanning calorimetry.[14] Because no signal was observed at GCE in the buffer containing $[C_{1,1,1,1}N][BF_4]$, i.e., $[C_{1,1,1,1}N][BF_4]$ has little effect on the structure of HRP, $[C_{1,1,1,1}N]^+$ ranks first. For the three imidazolium-based cations, $[\text{Hmim}]^+$ at low levels (0.2 M) results in the largest signal (up to (2.52 ± 0.17) μA) (Figure 6B), indicating that its stabilizing ability is the worst among the three cations used ($[\text{Hmim}]^+$ is also the worst among all cations tested). This phenomenon can be explained as follows. The longer alkyl chain on the imidazole ring makes the imidazolium-based cations more hydrophobic, and the strong interaction between the hydrophobic alkyl chain and the hydrophobic moieties on HRP, together with the electrostatic interaction between the imidazolium cation and the carboxyl on HRP, affects the natural structure of HRP,[30] which results in an exposure of the electroactive center and thus facilitates the direct electrochemistry of HRP. A similar phenomenon has been reported on the effects of imidazolium cations on the catalytic activity and stability of *Penicillium expansum* lipase.[31] $[\text{Bmpi}]^+$, $[\text{Bmpyrr}]^+$, $[\text{Bmim}]^+$, and $[\text{Bpy}]^+$ have a similar structure, but their effect is different. This is possibly due to the difference of the charge density on nitrogen. In $[\text{Bmpi}]^+$ and $[\text{Bmpyrr}]^+$, the positive charge concentrates at the nitrogen, whereas in $[\text{Bmim}]^+$ and $[\text{Bpy}]^+$ it delocalizes over the ring. The delocalization of the positive charge makes $[\text{Bmim}]^+$ and $[\text{Bpy}]^+$ more hydrophobic and thus destabilizes the protein.[14]

The kosmotropic/chaotropic concepts, which are correlated with the viscosity B coefficient of the Jones–Dole equation,[32] have been introduced to characterize the Hofmeister effect of simple inorganic ions. By analogy, the aforementioned series for IL cations is in the order of the relative increase of the kosmotropicity or of the relative decrease of the chaotropicity, for the more kosmotropic cations destabilize proteins in the Hofmeister effect of inorganic ions.

Figure 7 shows the effect of different $[\text{Bmim}]^+$-based ILs on the anodic peak current of HRP. At a level of 0.2 M IL, all ILs except $[\text{Bmim}]\text{Cl}$ and $[\text{Bmim}]\text{Br}$ result in an obvious current signal. For a given IL, the anodic peak current of HRP at GCE increases with the increase of its concentration. In terms of the stability of HRP, the Hofmeister series for the anions are

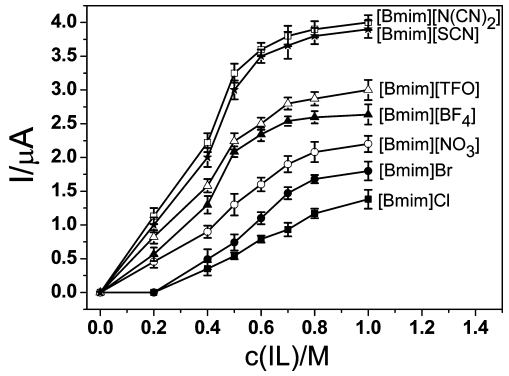

Figure 7. Effect of the concentrations of different anions on the anodic peak currents of HRP at the GCE. The concentration of HRP in the electrolyte was 50 μM and the incubation time at each IL concentration was 60 min. Scan rate: 1.0 V s^{-1}.

$$Cl^- > Br^- > [NO_3]^- > [BF_4]^- > [\text{TFO}]^- > [\text{SCN}]^- \approx [N(CN)_2]^-$$

Relatively speaking, the chaotropicity of the anions in the series is increased or the kosmotropicity decreased. It is known that the kosmotropic anions can strip off the water molecules originally associated with the protein molecule. That means the kosmotropic anions are able to decrease the protein surface area exposed to the solvent and thus maintains its natural structure.[33] For the chaotropic anions, however, they have not only a low water affinity but also a high polarizability, preferring to bind with the protein–water interface and thus destabilize the protein.[30] By comparison with the cations, the Hofmeister effects of some anions on the anodic peak current of HRP are bigger. This is because there are four positively charged amino acid residues (Arg31, Arg38, Lys147 and His 170) but no negatively charged ones around the active center of HRP.[34] The effect of the anions on the microenvironment around the active center is therefore more obvious than that of the cations.

■ CONCLUSIONS

The effects of different ILs on the structural stability of HRP, a model oxidoreductase, were systematically investigated using electrochemical methods. The redox signal at GCE is from the heme of HRP. An IL has a perturbing effect on the HRP structure, depending on its structure and its concentration. The

dx.doi.org/10.1021/jp3054263 | J. Phys. Chem. B 2012, 116, 11075–11080

electrostatic and hydrophobic interactions between HRP and GCE confine HRP to the surface of GCE and therefore facilitate the direct electrochemistry of HRP at GCE. Different cations or anions at varied concentrations have different effects on the structural stability of HRP, leading to different direct electron transfer currents at GCE. The anodic peak current of HRP at GCE, the catalytic activity of HRP, and the secondary structure of HRP are well correlated. The current signals in the presence of different ions can therefore be used as an indicator to quantitatively characterize the influencing ability of the ions on the structural stability of HRP. The present Hofmeister series for cations and anions is in good agreement with that reported elsewhere. To our knowledge, this is a first attempt to establish a simple and practical electrochemical method to correlate Hofmeister effects with characteristics of ions and solvents.

■ ASSOCIATED CONTENT

Supporting Information

The influence of 3.0 M guanidine hydrochloride on the electrochemical signal and the structure of HRP in the phosphate buffer (pH 7.0) is included. This information is available free of charge via the Internet at http://pubs.acs.org.

■ AUTHOR INFORMATION

Corresponding Author

*Phone: +86-531-88365433. Fax: +86-531-88365433. E-mail: xrhuang@sdu.edu.cn.

Notes

The authors declare no competing financial interest.

■ ACKNOWLEDGMENTS

The authors gratefully acknowledge the financial support from State Key Laboratory of Microbial Technology of China, the National Natural Science Foundation of China (Grant Nos. 20973103 and 21173133), the National Basic Research Program of China (Grant No. 2011CB707400), and the Graduate Independent Innovation Foundation of Shandong University (Grant No. yzc12066).

■ REFERENCES

(1) Hofmeister, F. *Arch. Exp. Pathol. Pharmakol.* **1888**, *24*, 247−260.
(2) von Hippel, P. H.; Wong, K. -Y. *Science* **1964**, *145*, 577−580.
(3) Kunz, W.; Lo Nostro, P.; Ninham, B. W. *Curr. Opin. Colloid Interface Sci.* **2004**, *9*, 1−18.
(4) Zhao, H. *J. Mol. Catal. B: Enzym.* **2005**, *37*, 16−25.
(5) Constatinescu, D.; Herrmanna, C.; Weingärtner, H. *Phys. Chem. Chem. Phys.* **2010**, *12*, 1756−1763.
(6) Shu, Y.; Liu, M.; Chen, S.; Chen, X.; Wang, J. *J. Phys. Chem. B* **2011**, *115*, 12306−12314.
(7) Heller, W. T.; O'Neill, H. M.; Zhang, Q.; Baker, G. A. *J. Phys. Chem. B* **2010**, *114*, 13866−13871.
(8) de María, P. D. *Angew. Chem., Int. Ed.* **2008**, *47*, 6960−6968.
(9) Wang, S.; Amornwittawat, N.; Banatlao, J.; Chung, M.; Kao, Y.; Wen, X. *J. Phys. Chem. B* **2009**, *113*, 13891−13894.
(10) Rehmann, L.; Ivanova, E.; Ferguson, J. L.; Gunaratne, H. Q. N.; Seddon, K. R; Stephens, G. M. *Green Chem.* **2012**, *14*, 725−733.
(11) Zhao, H.; Campbell, S. M.; Jackson, L.; Song, Z.; Olubajo, O. *Tetrahedron: Asymmetry* **2006**, *17*, 377−383.
(12) Rodrigues, J. V.; Prosinecki, V.; Marrucho, I.; Rebelo, L. P. N.; Gomes, C. M. *Phys. Chem. Chem. Phys.* **2011**, *13*, 13614−13616.
(13) Bekhouche, M.; Blum, L. J.; Doumèche, B. *J. Phys. Chem. B* **2012**, *116*, 413−423.
(14) Constantinescu, D.; Weingärtner, H.; Herrmann, C. *Angew. Chem., Int. Ed.* **2007**, *46*, 8887−8889.
(15) Shiddiky, M. J. A.; Torriero, A. A. J. *Biosens. Bioelectron.* **2011**, *26*, 1775−1787.
(16) Lu, L.; Huang, X.; Qu, Y. *Colloid Surf. B* **2011**, *87*, 61−66.
(17) Du, P.; Liu, S.; Wu, P.; Cai, C. *Electrochim. Acta* **2007**, *52*, 6534−6547.
(18) DiCarlo, C. M.; Compton, D. L.; Evans, K. O.; Laszlo, J. A. *Bioelectrochemistry* **2006**, *68*, 134−143.
(19) Smulevich, G.; English, A. M.; Mantini, A. R.; Marzocchi, M. P. *Biochemistry* **1991**, *30*, 772−779.
(20) Fujita, K.; MacFarlane, D. R.; Forsyth, M. *Chem. Commun.* **2005**, 4804−4806.
(21) Qiu, H.; Lu, L.; Huang, X.; Zhang, Z.; Qu, Y. *Bioresour. Technol.* **2010**, *101*, 9415−9520.
(22) Thongsook, T.; Whitaker, J. R.; Smith, G. M.; Barrett, D. M. *J. Agric. Food Chem.* **2007**, *55*, 1009−1018.
(23) Arai, K.; Hagiwara, S.; Takayama, S.; Murase, K.; Hirato, T.; Awakura, Y. *Electrochem. Commun.* **2006**, *8*, 609−614.
(24) Loget, G.; Chevance, S.; Poriel, C.; Simonneaux, G.; Lagrost, C.; Berthelot, J. R. *ChemPhysChem* **2011**, *12*, 411−418.
(25) Yang, J. T.; Wu, C. -S. C.; Martinez, H. M. *Methods Enzymol.* **1986**, *30*, 208−269.
(26) Wei, W.; Danielson, N. D. *Biomacromolecules* **2011**, *12*, 290−297.
(27) Weaver, K. D.; Vrikkis, R. M.; Vorst, M. P. V.; Trullinger, J.; Vijayaraghavan, R.; Foureau, D. M.; McKillop, I. H.; MacFarlane, D. R.; Krueger, J. K.; Elliott, G. D. *Phys. Chem. Chem. Phys.* **2012**, *14*, 790−801.
(28) Rahimi, P.; Rafiee-Pour, H.; Ghourchian, H.; Norouzi, P.; Ganjali, M. R. *Biosens. Bioelectron.* **2010**, *25*, 1301−1306.
(29) Wang, J. *Analytical Electrochemistry*: VCH, New York, 1999, p 38.
(30) Yang, Z. *J. Biotechnol.* **2009**, *144*, 12−22.
(31) Lai, J.; Li, Z.; Lu, Y.; Yang, Z. *Green Chem.* **2011**, *13*, 1860−1868.
(32) Jones, G.; Dole, M. *J. Am. Chem. Soc.* **1929**, *51*, 2950−2964.
(33) Collins, K. D.; Neilson, G. W.; Enderby, J. E. *Biophys. Chem.* **2007**, *128*, 95−104.
(34) Berglund, G. I.; Carlsson, G. H.; Smith, A. T.; Szöke, H.; Henriksen, A.; Hajdu, J. *Nature* **2002**, *417*, 463−468.